Molecular Cell, Vol. 14, 269–276, April 23, 2004, Copyright ©2004 by Cell Press

Structural Basis for Dimerization of ICAM-1 on the Cell Surface

Short Article

Yuting Yang,[1,3,8,9] Chang-Duk Jun,[2,4,8,10] Jin-huan Liu,[1,3] Rongguang Zhang,[7] Andrzej Joachimiak,[7] Timothy A. Springer,[2,4,*] Jia-huai Wang[1,5,6,*]
[1]Dana-Farber Cancer Institute
[2]Center for Blood Research
Boston, Massachusetts 02115
[3]Department of Medicine
[4]Department of Pathology
[5]Department of Pediatrics
[6]Department of Biological Chemistry and Molecular Pharmacology
Harvard Medical School
Boston, Massachusetts 02115
[7]Biosciences Division
Argonne National Laboratories
Argonne, Illinois 60439

Summary

We have determined the 3.0 Å crystal structure of the three C-terminal domains 3–5 (D3–D5) of ICAM-1. Combined with the previously known N-terminal two-domain structure (D1D2), a model of an entire ICAM-1 extracellular fragment has been constructed. This model should represent a general architecture of other ICAM family members, particularly ICAM-3 and ICAM-5. The observed intimate dimerization interaction at D4 and a stiff D4–D5 stem-like architecture provide a good structural explanation for the existence of preformed ICAM-1 *cis* dimers on the cell membrane. Together with another dimerization interface at D1, a band-like one-dimensional linear cluster of ICAM-1 on an antigen-presenting cell (APC) surface can be envisioned, which might explain the formation of an immunological synapse between an activated T cell and APC which is critical for T cell receptor signaling.

Introduction

The intercellular adhesion molecule-1 (ICAM-1, CD54) is a type I transmembrane glycoprotein composed of five immunoglobulin superfamily (IgSF) domains, a hydrophobic transmembrane segment, and a short cytoplasmic tail (Staunton et al., 1990). ICAM-1 is expressed at basal levels on immune system and endothelial cells, and is greatly upregulated by inflammatory mediators in response to immune challenge. Increased ICAM-1 expression augments the immune response and leukocyte accumulation in inflamed tissues. ICAM-1 is a ligand for leukocyte integrins (Springer, 1990). Integrins are a family of heterodimeric transmembrane cell adhesion molecules consisting of noncovalently associated α and β chains. The two leukocyte integrins that bind to ICAM-1 are $\alpha_L\beta_2$ (LFA-1, CD11a/CD18) and $\alpha_M\beta_2$ (Mac-1, CD11b/CD18). $\alpha_L\beta_2$ binds to ICAM-1 domain 1, whereas $\alpha_M\beta_2$ binds domain 3. The binding is through the integrin α chain's I domain to an acidic residue on ICAM-1. Multimeric ligand binding triggers signal transduction inside the cell (reviewed in Hynes, 2002; Springer, 1990). Crystal structures of the N-terminal two-domain fragment of ICAM-1 (Bella et al., 1998; Casasnovas et al., 1998) and its complex with the $\alpha_L\beta_2$ I domain (Shimaoka et al., 2003) reveal an atomic resolution image of the two Ig-like domains of ICAM-1 and how binding to the I domain is regulated by and conversely can also induce conformational changes of the latter. These structural data begin to unravel the mechanism of ICAM-1-mediated cell adhesion at the molecular level, which is of particular immunological significance.

In addition to ICAM-1, another four major ICAM family members (ICAM-2, -3, -4, and -5) are known to be ligands for leukocyte integrins. They differ in their expression patterns and the number of constituent domains. Except for ICAM-4, they all appear to bind to the $\alpha_L\beta_2$ I domain through a key acidic residue in their domain 1 (Gahmberg, 1997). Although each ICAM family member has its own unique biological function, as the most widely distributed and important one, ICAM-1 serves as a paradigm in the investigation of the structure and function of the ICAM family.

Here we report a 3.0 Å resolution crystal structure of a fragment containing the three C-terminal domains (D3–D5) of ICAM-1, which allows us, in conjunction with the previously known ICAM-1 D1D2 structure, to construct an entire extracellular fragment of ICAM-1. This makes it possible to envisage how all ICAM family members may be formulated. More interestingly, the observation of molecular dimerization in this ICAM-1 D3–D5 crystal structure provides a structural basis for the existence of the biologically relevant, dimeric form of ICAM-1 molecules on the cell surface (Miller et al., 1995; Reilly et al., 1995). Along with the D1–D1 dimer in the ICAM-1 D1D2 structure, we discuss a possible explanation of how an immunological synapse (Grakoui et al., 1999; Lee et al., 2003) might be formed.

Results

The Structure of D3–D5

To determine the structure of ICAM-1 D3–D5, a construct containing Phe185 to Pro450 was expressed in lectin-resistant CHO Lec.3.2.8.1 cells. The protein was antibody-affinity purified and deglycosylated with Endo H before crystallization. The crystal accommodates two molecules in an asymmetric unit. The structure was solved using conventional multiple isomorphous replacement (Table 1).

The structure of ICAM-1 D3–D5 (Figure 1) shows that all three domains can be classified as IgSF domains, although D4 and D5 have unusual features. Like other

*Correspondence: springer@cbr.med.harvard.edu (T.A.S.); jwang@red.dfci.harvard.edu (J.-h.W.)
[8]These authors contributed equally to this work.
[9]Present address: Rosenstiel Center, Brandeis University, Waltham, Massachusetts 02454.
[10]Present address: Department of Microbiology and Immunology, Wonkwang University School of Medicine, Chonbuk 570-749, Korea.

Table 1. Crystallographic Statistics

	Native	Os Derivative	Pt Derivative
Space group	R32		
Unit cell	a = b = 193.7, c = 175.3	a = b = 193.3, c = 174.1	a = b = 193.0, c = 172.7
Resolution (Å)	3.0	3.0	3.1
Reflections (overall/unique)	404,143/25,310	360,064/25,575	492,935/22,102
R_{sym} (%)	12.5	10.1	10.8
I/sigma (overall/last shell)	I0.9/3.1	18.1/3.7	23.3/3.6
Completeness (overall/last shell; %)	100/100	100/99.8	96.7/97.1
Structure Determination			
R_{iso} (%)		15.0	18.7
Number of sites		4	2
Phasing power (centric/acentric)		1.01/0.89	0.81/0.71
R_{cullis} (centric/acentric)		0.61/0.84	0.65/0.89
FOM	0.30		
Refinement			
Refinement range (Å)	20−3.0		
Data cutoff (|F|)	0.0		
No. of reflections (work/test)	20,492/2262		
R_{cryst}/R_{free} (%)	22.2/25.5		
Ramachandran statistics (%) (good/ additional/generous/forbidden)	90.2/9.6/0.2/0.0		
Protein atoms average B value (Å^2)	35.2		
Rmsd bond lengths (Å)/angles (°)	0.008/1.37		

concatenated IgSF structures, an obtuse twist angle between successive domains causes an alternation in the domains' exposed faces (Wang and Springer, 1998). In addition, a sharp bend of ~140° is observed between the long axes of domains D3 and D4, whereas the axes of D4 and D5 are almost aligned. There are four potential N-glycosylation sites, of which only three were identified in electron density maps to have sugar moieties, two on D3 and one on D4 (Figure 1). The fourth site at Asn379 on D5 is not utilized, probably because of the unfavorable presence of a Trp in the Asn-Trp-Thr N-glycosylation sequon.

D3 falls into the I1 subset of IgSF domains (Wang and Springer, 1998). It is made up of two β sheets containing the ABED and A′GFCC′ β strands, respectively, similar to ICAM-1 D1. An unusual characteristic of D3 for IgSF domains is its relatively long DE loop. Interestingly, at the very tip of the DE and the FG loops, there is one glycan each linked to Asn240 and Asn269, respectively, both pointing up (Figure 1). Were domain 2 present, these two glycans would flank the bottom of D2 and thus constrain interdomain movement at the D2–D3 junction. Mutation data showed (Diamond et al., 1991) that the key $\alpha_M\beta_2$ binding residue is Asp229, located on the protruding CD loop in D3 (Figure 1). By contrast, the critical $\alpha_L\beta_2$ binding residue, Glu34, is at the end of strand C of D1, on a relatively flat surface (Shimaoka et al., 2003). A mutation removing the glycan at Asn269, as well as decreasing the amount of the N-linked carbohydrate in general on ICAM-1, markedly augmented $\alpha_M\beta_2$ binding

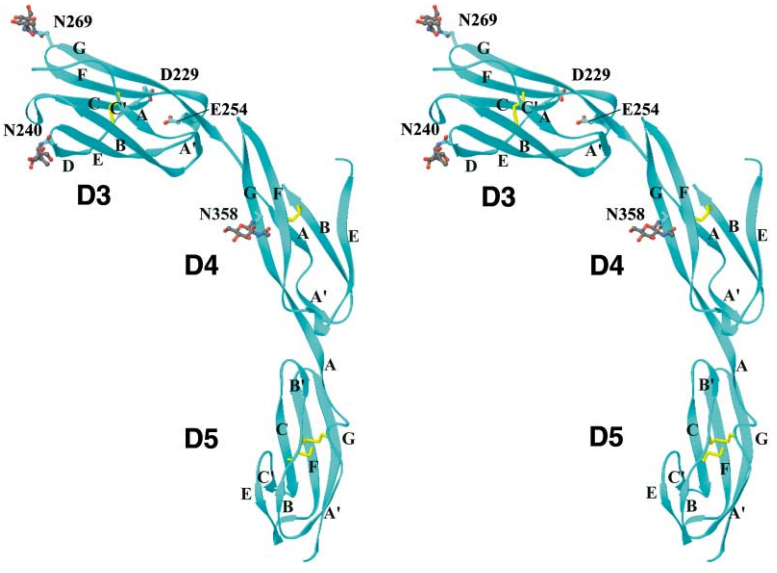

Figure 1. The Ribbon Drawing of ICAM-1 Domain 3–5 Fragment in Stereo

In this drawing, β strands are all labeled, and the key $\alpha_M\beta_2$ binding site Asp229, another important binding residue Glu254, and three glycans are shown in ball-and-stick representation. The disulfide bonds are in yellow. Note that in D5 two disulfide bonds are formed within each β sheet, the E strand is very short, and the AA′ loop has a unique helical conformation. Also note that in D4 the break between the B and E strands, where 16 missing residues are supposed to be, can be seen. The figure was prepared using the program RIBBONS (Carson, 1995).

but had little effect on $\alpha_L\beta_2$ binding (Diamond et al., 1991). The glycan at Asn269 is on the same face as Asp229. Therefore, eradicating the lengthy glycan must remove its shielding effect on the binding of $\alpha_M\beta_2$ at Asp229.

D4 appears to have only five β strands, ABE on one sheet and A′GF on the other (if A and A′ are counted as a single strand), as opposed to the seven to nine β strands of a typical IgSF domain. A peculiar feature of D4 is a long disordered region between the B and E strands, encompassing residues His308–Leu323. It is rare to have such a long floppy loop in a small domain. Secondary structure prediction of this region argues for a possible existence of a short stretch of β structure (data not shown). As described below, there is a large dimerization interface in D4. We suspect that when the ICAM-1 molecule is monomeric, the 16 residue-long disordered loop may fold into a BC loop, C strand, trace of C′ strand, C′E loop structure in a fashion similar to that seen in I2 set IgSF domains. However, ICAM-1 D4 is markedly shorter than other IgSF domains in this region. The counterpart regions in D2 of ICAM-1 (PDB code 1IC1), ICAM-2 (PDB code 1ZXQ), CD2 (PDB code 1HNF) and CD4 (PDB code 3CD4) are 28, 33, 22, and 23 residues long, respectively. We speculate that this relatively short 16 residue segment in ICAM-1 D4 has a tendency to unfold, becoming disordered, and enabling formation of the energetically and biologically more favorable D4–D4 "superdomain" dimer as discussed below.

D5 is a distorted I2 subset IgSF domain. D5 starts at Tyr367. The strand A of D5 is a continuation of strand G of D4 and is followed by a unique, protruding, highly charged 3_{10} helix-like AA′ loop (Figures 1 and 3C). Moreover, the E strand is just half the normal size. All of these result in an irregular ABE β sheet such that the central B strand breaks into B and B′ strands (Figure 1). Another unique structural aspect of D5 is that its four cysteines are clustered in the middle of the domain. Despite the fact that Cys392 on the B strand and Cys430 on the F strand are in positions almost suitable to form the canonical intersheet disulfide bond, electron density maps unambiguously show that these four cysteines actually pair into two intrasheet disulfide bonds within the domain, "elbow-to-elbow", between neighboring A and B strands in one sheet and between neighboring C and F strands in the other (Figure 1).

The Molecular Model of the Entire ICAM-1 Ectofragment

The availability of both domain 1–2 and domain 3–5 structures (the secondary structure assignment is shown in Figure 2) makes it possible to construct an entire extracellular fragment of ICAM-1. Single-molecule electron microscopic (EM) images have shown that the ICAM-1 molecule has a rod-like shape with a characteristic bend between D3 and D4 (Kirchhausen et al., 1993). This observation is consistent with the bend seen between D3 and D4 in our D3–D5 structure. We have noticed a charged hydrogen bond between Glu201 of domain 3 and Lys357 of domain 4 where the molecule bends and also a large hydrophobic patch on the other side of the D3–D4 interface. This hydrophobic interface actually extends into the hydrophobic core of D4. These interactions stabilize the bend. Our model of the D2–D3 interface is consistent with EM images, which imply that the D2–D3 linkage is relatively straight.

Phe185 is the last residue of D2 in the D1D2 structure (Bella et al., 1998; Casasnovas et al., 1998), and the subsequent Val186, the first residue in our D3–D5 structure, has two main chain hydrogen bonds to Phe216 on the BC loop of D3 in the D3–D5 structure. Immediately following Phe216 is a conserved *cis*-Pro217. This structural characteristic renders Val186 a typical pivot residue, i.e., a residue at which the adjacent domains have limited flexibility, as seen in many other IgSF structures (Wang and Springer, 1998). Therefore, the whole D1–D5 fragment model can be tentatively constructed (Figure 3A) in a manner as described in the Experimental Procedures. A D2–D3 interface with reasonable stereochemistry can be modeled (Figure 3B). On one side there might be a salt link between D2's Arg150 and D3's Asp241. On the other side of the interface, the first sugar moiety on D3's Asn269 might pack onto the indole ring of D2's Trp97 as commonly seen in glycoprotein structures. In the center, the pivotal residue Val186, the conserved *cis*-Pro217 and the Phe216 in D3's BC loop along with a group of hydrophobic residues could comprise a cushion-like interface (Wang and Springer, 1998). In Figure 3A the ICAM-1 molecule is oriented as if it stands on the cell surface. In this configuration, the important $\alpha_M\beta_2$ binding residues Asp229 and Glu254 on D3 pose for integrin binding from the opposing cell. Meanwhile, the key $\alpha_L\beta_2$ binding residue Glu34 and surrounding binding interface with the $\alpha_L\beta_2$ I domain (Shimaoka et al., 2003) are also in a favorable position for binding.

The sequence of the ICAM-1 cDNA was found to be distributed over seven exons (Voraberger et al., 1991). Remarkably, the boundaries between the five IgSF domains in the molecular three-dimensional structure exactly correspond to the introns between exons 2–6, whereas the first exon encodes the signal peptide and the seventh exon encodes the transmembrane segment plus cytoplasmic tail. This is a good example of how this kind of cell surface molecule might have evolved in a modular fashion.

Structural Alignment of ICAM Family Members

At least five members of the ICAM family have been well characterized (reviewed in Gahmberg, 1997). ICAM-3 is the most homologous of all to ICAM-1 with the same number of extracellular domains and high sequence similarity, whereas ICAM-5 has nine and ICAM-2 and ICAM-4 have only two domains on the cell surface, respectively. Here we will confine our comparison of ICAM-1 only to ICAM-3 and -5, because sequence-wise these three are most closely related and the genes encoding ICAM-3 and ICAM-5 are clustered in close vicinity to the ICAM-1 gene on human chromosome 19p13.2. These are clear indications that these family members may have arisen from a primordial ICAM through a gene duplication mechanism.

Figure 2 illustrates the sequence alignment of D1–D5 of ICAM-1 with the homologous domains of ICAM-3 (52% identical) and ICAM-5 (50% identity). Several interesting points can be seen in the figure. Structurally, all disulfide bonds are invariant. Key $\alpha_L\beta_2$ binding residues

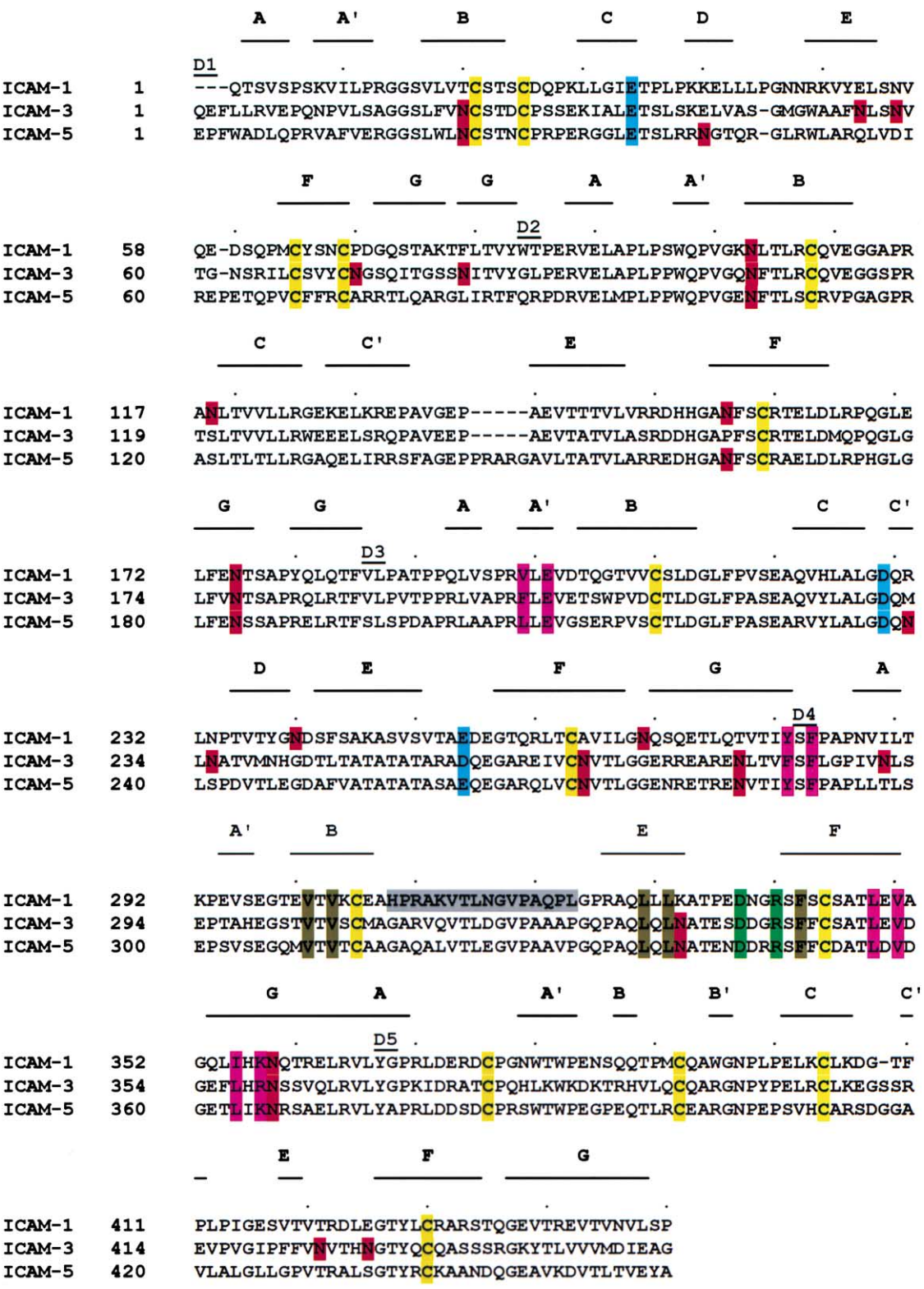

Figure 2. The Sequence Alignment of ICAM-1 with ICAM-3 and ICAM-5

As shown in the figure, ICAM-1, ICAM-3, and ICAM-5 align very well. The conserved residues include all cysteines (yellow), three integrin binding residues (cyan), those involved in the D4–D4 dimerization interface (residues forming a salt bridge are in green and hydrophobic contacts are in yellow-green), and those involved in the D3–D4 bending interface (magenta). In this figure, each domain's first residue is manifest with its label, β strands are marked above the ICAM-1 sequence, and every tenth residue is marked with a dot above the ICAM-1 sequence. In addition, glycosylation sites are colored in red, whereas the disordered 16 residues in D4 of the D3–D5 crystal structure are shaded in gray.

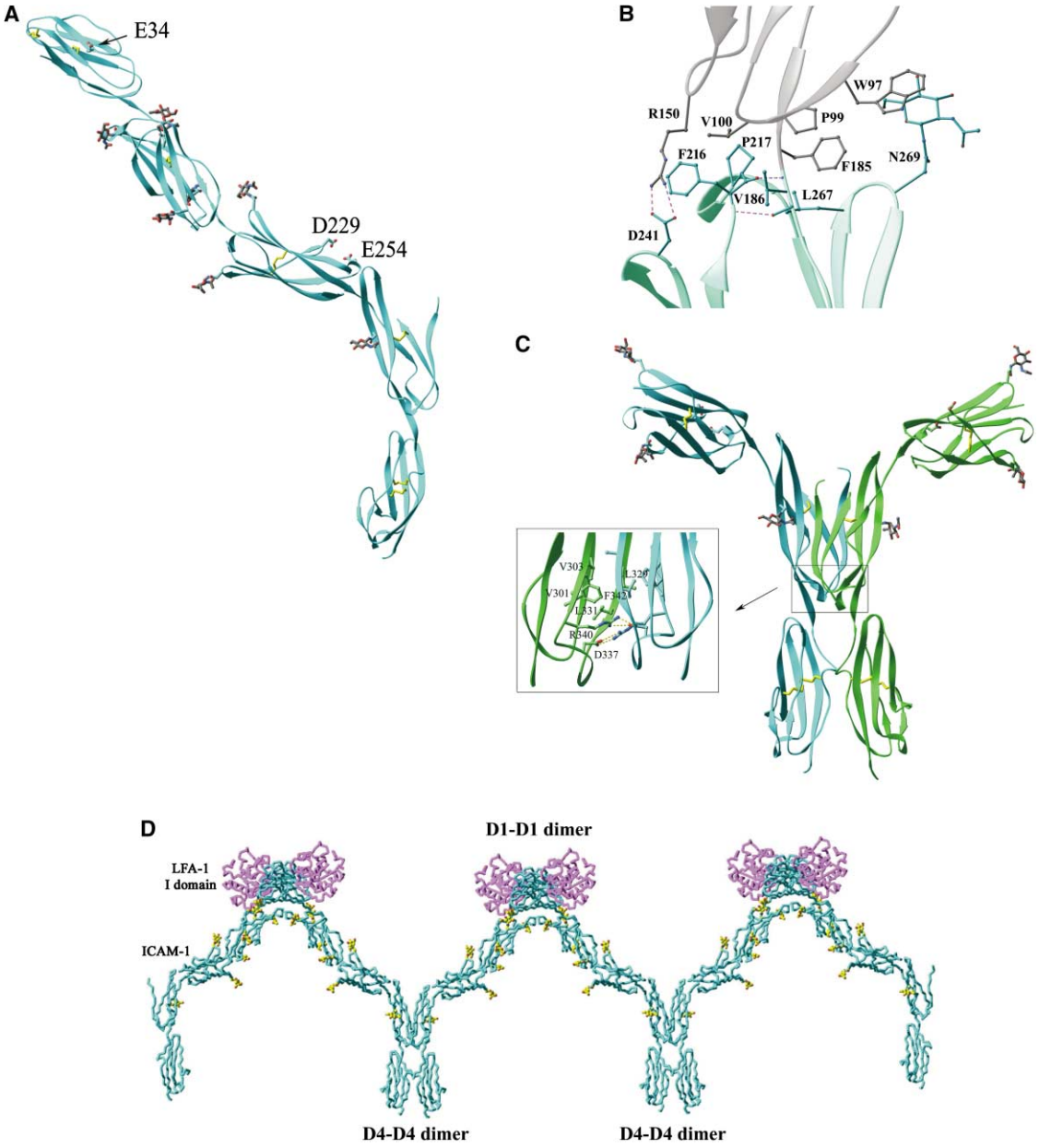

Figure 3. The Molecular Structure of the Entire ICAM-1 Ectofragment and the ICAM-1 Dimer

(A) This ICAM-1 D1–D5 model was constructed by linking the known D1D2 structure and the D3–D5 structure reported here at the pivot residue Val186 as described in the Experimental Procedures. Assuming that D5 stands vertically on the cell membrane, both the key $\alpha_L\beta_2$ binding site Glu34 of D1 and the $\alpha_M\beta_2$ binding sites Asp229 and Glu254 of D3 (all shown in ball-and-stick representation) point upward, available for ligand binding from the opposing cell above. Note that the Glu34 is on a relatively flat surface, whereas the Asp229 is on a protruded loop. All seven identified glycans are shown in ball-and-stick representation (prepared with RIBBONS [Carson, 1995]).

(B) This is the modeled D2–D3 interface. Domains 2 and 3 are colored in silver and cyan, respectively. Shown here are only the side chains that contribute to the interface. The broken lines depict a salt link between Arg150 of D2 and Asp241 of D3. On the other side of the interface the sugar moiety on D3's Asn269 packs onto the indole ring of D2's Trp97. At the center, two main chain hydrogen bonds are formed between the pivot Val186 and Phe216 in D3's BC loop. Joining them is a group of hydrophobic residues, including the conserved *cis*-Pro217, that comprise a cushion (Wang and Springer, 1998) (prepared with RIBBONS [Carson, 1995]).

(C) In this D3–D5 dimer drawing, one molecule is in cyan and the other in green, while disulfide bonds are in yellow. Glycans are drawn in ball-and-stick representation. The two molecules have their D4s integrated into a "superdomain." In the inset, extensive hydrophobic contacts in the D4–D4 interface are seen, which include Val301, Val303, Leu329, Leu331, and Phe342 from each molecule. There are also two pairs of charged hydrogen bonds between one molecule's Arg340 and its dyad-mate's Asp337 and vice versa. The view in the inset is flipped 180° vertically for clarity (prepared with RIBBONS [Carson, 1995]).

(D) In this drawing, ICAM-1 D1–D5 molecules form D4–D4 dimer, and D4–D4 dimers come together through D1–D1 contacts. The W-shaped tetramers can further propagate into a band-like one-dimensional cluster on the antigen-presenting cell surface. The $\alpha L\beta 2$ I domain (magenta) binds to ICAM-1 D1 at the opposite face of D1–D1 dimerization. The glycans on ICAM-1 are in yellow (prepared with RIBBONS [Carson, 1995]).

are conserved. Not only the $\alpha_L\beta_2$ binding residue, Glu34, but those residues important for $\alpha_M\beta_2$ binding, Asp229 and Glu254, are also conserved, although currently there are no experimental data suggesting that $\alpha_M\beta_2$ binds to ICAM-3 or ICAM-5. Intriguingly, those residues thought to be the determinants in ICAM-1 D2–D3 bending and D4–D4 dimerization that will be discussed below are also quite conserved. One could predict that the characteristic bend in the D2–D3 junction and the D4-mediated dimerization might be present in all three ICAM family members.

ICAM-5 has four further C-terminal IgSF domains, which are not shown in Figure 2. Among the four, only the ninth domain is distinct while domains 6 to 8 are homologous to domain 5, including the presence of the two unusual intrasheet disulfide bonds in the core. The molecular structure of ICAM-1 presented here hence suggests a modular architecture of A-B-A-B-C for ICAM-1 and ICAM-3, and A-B-A-B-C-C-C-C-D for ICAM-5, with A and B being I1 and I2 set IgSF domains, C a unique I2 set, and D a distinct one, respectively. ICAM-1 is widely expressed in different tissues. On the contrary, ICAM-3 and ICAM-5 have restricted expression, and ICAM-5 is highly basic with 15 arginines in D1 (Figure 2). Obviously, although they all bind to $\alpha_L\beta_2$, these ICAMs have evolved to divert their roles in different biological settings. Since ICAM-3 is the principal $\alpha_L\beta_2$ ligand on resting leukocytes, this led to the speculation that it might play a role in the initiation of immune responses (de Fougerolles and Springer, 1992; Fawcett et al., 1992; Vazeux et al., 1992). ICAM-5 is exclusively expressed in the telencephalon of the mammalian brain. The $\alpha_L\beta_2$/ICAM-5 interaction mediates T cell binding to hippocampal neurons (Gahmberg, 1997). The molecular structure of ICAM-1 presented here should provide a good framework for studying the homologs ICAM-3 and ICAM-5 at the molecular level.

The Intimate Dimer

One striking feature of the ICAM-1 D3–D5 crystal structure is the manner whereby the two molecules dimerize in a Y shape (Figure 3C). The two protomers come into such intimate contact in D4 that the two D4s actually merge into an integrated structure with two super β sheets of ABE−FGA′ (the ABE from one D4 and the FGA′ from the pseudo-dyad related D4) facing each other around the pseudo-dyad. The E strand of one D4 runs antiparallel to the F strand of the other D4 such that the segment of Arg326–Leu330 of the E strand of one D4 pairs to the segment Thr347–Ser343 of the F strand of the other D4, forming six main chain hydrogen bonds in each super sheet. This hydrogen bond network is located at the upper portion of the domain. In the middle of the dimer interface, hydrophobic residues Val301, Val303, Leu329, Leu331, and Phe342 from each protomer cluster together. Near the bottom of the domain, an Arg340 of one protomer salt links to the other protomer's Asp337 and vice versa, adding four more charged hydrogen bonds. These quite extensive interactions, hydrophobic in the center and hydrophilic at both ends, almost span the whole domain (Figure 3C, inset), burying a total of about 1930 Å^2 solvent accessible surface area. This makes the D4–D4 region just like a single domain.

The merge of two D4s brings the two D5s close. Since the β sheets of the two D4s are on the same plane, the relative twist between domains D4 and D5 orients two D5s such that their ABE sheets more or less face each other with their uniquely protruded AA′ loops in contact (Figure 3C). The long and positively charged side chain of Arg374 at the tip of one D5's AA′ loop approaches Asp372 and Asp375 of its symmetry-mate. Furthermore, the stiff interdomain connection provided by the continuation of strand G of D4 into strand A of D5 assures that the two D5s vertically align with the D4–D4 superdomain, giving rise to a stem-like architecture at the C-terminal end of the ICAM-1 dimer.

The observed intimate dimerization at D4 and the stem-like dimeric D4–D5 structural arrangement is in agreement with data showing that ICAM-1 molecules are present on the cell surface in dimeric form (Miller et al., 1995; Reilly et al., 1995). These authors used a variety of methods including chemical crosslinking to show that the majority of ICAM-1 molecules are dimeric on the cell surface. Furthermore, monoclonal antibody CA7 was found to bind monomeric but not dimeric ICAM-1 (Miller et al., 1995). The CA7 epitope maps to D5, consistent with D5 being close together in the dimer as seen in our structure. These authors also demonstrated that when ICAM-1 is expressed in a glycolipid-anchored form it is primarily monomeric. Since an ICAM-1 cytoplasmic tail deletion mutant was still dimeric, these experiments imply that the transmembrane portion of ICAM-1 aids dimerization (Miller et al., 1995). In our D4–D5 stem-like arrangement, the C termini of two ICAM-1 molecules are juxtaposed near the membrane, consistent with association between their transmembrane α helices. Presumably, D4–D4 dimerization on the cell surface would require a local unfolding of the 16 residues between the C and E strands, which would cost energy. This may explain why the transmembrane portion aids dimerization and recombinant soluble ICAM-1 molecules do not dimerize (Miller et al., 1995; Reilly et al., 1995). In conclusion, our crystal structure of ICAM-1 D3–D5 has provided a structural basis for dimerization of ICAM-1 on the cell surface.

Discussion

The Integrin Binding Site Presentation

Important points can be addressed which are pertinent to the ICAM-1 dimer on the cell surface. Properly orienting an elongated molecule like ICAM-1 on the cell surface is important for optimal exposure of its ligand binding site in *trans*. The issue is particularly relevant if one considers that these molecules function on the endothelial surface and will experience force exerted by blood flow (Wang and Springer, 1998). In the case of ICAM-2, three uniformly distributed glycans on the membrane-proximal domain 2 were suggested to function like a tripod to hold the molecule "standing" on the cell surface, facilitating ligand binding site presentation (Wang and Springer, 1998). Similarly, the Y-shaped ICAM-1 dimer and the rigid dimerized D4–D5 stem provide a structural solution to the problem of optimally orienting the ligand binding sites in D1 and D3. As described earlier, the key $\alpha_M\beta_2$ binding residue is the Asp229 on the pro-

truded CD loop of D3 and the nearby Glu254 on the EF loop of the same domain is also important for binding to $\alpha_M\beta_2$ (Diamond et al., 1991). The Asp229 and Glu254 are on the same face of each arm of a Y-shaped dimer and posed up toward the opposing cell (Figure 3A). Since D1 is roughly in a similar orientation as D3, the $\alpha_L\beta_2$ binding site on D1 will also be favorably oriented (Figure 3A).

The Band-like One-Dimensional Clustering of ICAM-1s and the Immunological Synapse

The ICAM-1 D1 also mediates dimerization as shown in both the ICAM-1 D1D2 structure (Casasnovas et al., 1998) and the structure of ICAM-1 D1D2/$\alpha_L\beta_2$ I domain complex (Shimaoka et al., 2003). These D1–D1 dimers are similar in having an interface centered at Leu18. However, they bury only half as much surface area as the D4–D4 dimer. Moreover, the D4 interface, but not D1 interface, would bury the CA7 epitope as observed for ICAM-1 dimer on the cell surface (Miller et al., 1995). Therefore, we believe that D4–D4 dimerization, the D4–D5 stem-like configuration, and additional contribution from amphipathic transmembrane helices are responsible for the preformed ICAM-1 dimers present on the cell surface. Visualization with EM of the soluble ICAM-1 D1–D5 (sICAM-1) molecules, which are forced to dimerize through a disulfide-linked leucine zipper fused C-terminal to D5, showed mostly extended dimmers (Jun et al., 2001b). Interestingly there were also small amounts of U-like (dimerized at D4–D4) and O-like dimers (D4–D4 and D1–D1 contacts within one dimer) and W-shaped tetramers (D1–D1 contacts connect two D4–D4 dimers) (Figure 3D), indicating that the D1–D1 interaction, albeit significantly weaker, indeed exists in solution (Jun et al., 2001a). Together, dimerization at the D4–D4 and D1–D1 interfaces should facilitate the formation of a W-shaped tetramer, in agreement with EM observations (Jun et al., 2001a), and chain-like propagation of further ICAM-1 molecules would result in a continuous band-like one-dimensional cluster on the cell surface (Figure 3D).

Dustin and colleagues reported real-time imaging and quantitative analysis of the formation of a functional immunological synapse (Grakoui et al., 1999). Although the biological significance of an immunological synapse is controversial, the most recent consensus is that the immunological synapse helps to regulate T cell signaling (Huppa and Davis, 2003; Lee et al., 2003). One key feature of a mature immunological synapse lies in its topology which maintains an adequate intermembrane distance between the T cell and the APC, having shorter adhesion molecular pairs, such as CD2/CD58, in the central zone and longer adhesion pairs of ICAM-1/$\alpha_L\beta_2$ in the periphery (Springer, 1990). The signaling TCR/pMHC pairs are short in size, thereby fitting well into the central zone (Grakoui et al., 1999).

The constructed band-like one-dimensional ICAM-1 cluster presented here, in conjunction with the complex structure of the ICAM-1 D1D2/$\alpha_L\beta_2$ I domain (Shimaoka et al., 2003) offers a plausible model for immunological synapse formation. The band-like ICAM-1 molecules shown in Figure 3D can propagate into a one-dimensional cluster on the APC surface, and integrin $\alpha_L\beta_2$ molecules can reach from the opposing T cell, binding to ICAM-1 D1. This zigzagged band created by ICAM-1 can close up, forming a circle. There is evidence that upon binding to leukocytes, ICAM-1 molecules on the endothelial surface are rapidly relocalized and the endothelium proactively forms an ICAM-1-enriched cup-like structure that surrounds adherent leukocytes (Carman et al., 2003). The $\alpha_L\beta_2$ engagement and the known specific interaction of ICAM cytoplasmic tails with ezrin/radixin/moesin proteins, which further associate with actin bundles in microvilli (Hamada et al., 2003), probably facilitate the concentration of preformed ICAM-1 dimers on the endothelium to develop into a one-dimensional band-like structure. It is conceivable that when two opposing cells come into contact, eventually the one-dimensional ICAM-1/$\alpha_L\beta_2$ cluster on the periphery could encircle the two-dimensional cluster of immune molecules in the central zone to create a mature immunological synapse. One interesting fact is that despite the conservation of those residues in the D4–D4 interface in other ICAM family members, potential glycosylation sites on the D1–D1 interface in ICAM-3 and ICAM-5 (see the common Asn-Cys-Ser N-glycosylation sequon on D1's B strands for these two ICAMs in Figure 2, and probably other sites on the D and E strands) would prevent them from dimerizing at D1. Therefore, ICAM-1 may have a predominant role in synapse formation.

Experimental Procedures

Protein Preparation and Crystallization

A construct of the ICAM-1 domain 3–5 fragment (Phe185–Pro450) was made by mutating the cDNA of ICAM-1. The entire transmembrane and cytoplasmic domain of ICAM-1 was deleted by transforming the codon for the residue Arg451 to a translational stop codon. The D1–D2 fragment was deleted using long (45 bp) mutant oligonucleotides to span the distal ICAM-1 sequence such that codons for the end of the signal sequence and Phe185 would be joined. The PCR product was inserted into the pBJ5-GS vector. The CHO.Lec3.2.8.1 cell transfectants were selected, and the ICAM-1 D3–D5 fragment expressed by a stable cell line was purified by immunoaffinity with the CBR-IC1/11 monoclonal antibody. The purified protein was deglycosylated with Endo H and further purified by ion-exchange chromatography.

Crystals were grown using the vapor diffusion method in hanging drops at room temperature. Equal volumes of 15 mg/ml protein solution and the reservoir solution of 1 M $NH_4H_2PO_4$/0.1 M Na-citrate (pH 5.6) were mixed. The grown crystals were transferred to a cryoprotectant buffer containing 20% PEG 4K (w/v), 0.1 M Na-citrate (pH 5.6), and 20% (v/v) glycerol for freezing in liquid nitrogen.

Structure Determination and Refinement

Structure was determined using the MIR method with heavy atom derivatives of K_2PtCl_4 and K_3OsCl_6 (both at 1 mg/ml concentration). All data were collected near −160°C at APS SBC 19ID beamline in Argonne National Laboratories. Reflection data were indexed, integrated, and scaled using the program suite HKL2000 (Otwinowski and Minor, 1997). Heavy atom positions were located and phases were estimated with SOLVE (Terwilliger and Berendzen, 1999). The electron density map calculation and improvement were carried out with CNS (Brunger et al., 1998). A model was built manually with program O (Jones et al., 1991). The model refinements were done using the simulated annealing protocol implemented in CNS. The final model consists of two ICAM-1 molecules, each of which has disordered 16 residues (His308–Leu323) missing as stated before. One sugar moiety was included at each of the six N-glycosylation sites for the two molecules. The electron densities for the sugar residue at Asn240 site of molecule B were too weak for unambiguous

model building, and the current assignment is therefore a tentative one. Altogether, 65 water molecules were included in the model.

Model Construction of ICAM-1 Domain 1–5

Molecule A of the D1D2 crystal structure (PDB code 1ZXQ) was used to align its crystal dyad with the pseudo-dyad of the D3–D5 structure that relates the two independent molecules. This is roughly a 174° rotation of this D1D2 model about the horizontal axis. Translate the rotated D1D2 model so as to connect Phe185 of D1D2 to Val186 of D3–D5. Twist the D3 along its longest axis about 42° anticlockwise to make a more reasonable connection of D2–D3 and D3–D4 so that the twist angles between D2–D3 and D3–D4 are 116° and 129°, respectively. Make minor adjustment of interfaces for both D2–D3 and D3–D4. This D1–D5 model was used to build the W-shaped tetramer and band-like configuration (Figure 3D).

Acknowledgments

We thank Kemin Tan for his valuable help in early crystallographic work. We also thank Linda Clayton for critical reading. This work was supported by grant HL48675 from the NHLBI.

Received: December 27, 2003
Revised: March 4, 2004
Accepted: March 8, 2004
Published: April 22, 2004

References

Bella, J., Kolatkar, P.R., Marlor, C.W., Greve, J.M., and Rossmann, M.G. (1998). The structure of the two amino-terminal domains of human ICAM-1 suggests how it functions as a rhinovirus receptor and as an LFA-1 integrin ligand. Proc. Natl. Acad. Sci. USA *95*, 4140–4145.

Brunger, A., Adams, P., Clore, G., DeLano, W., Gros, P., Grosse-Kunstleve, R., Jiang, J.-S., Kuszewski, J., Nilges, N., Pannu, N., et al. (1998). Crystallography & NMR system (CNS): a new software system for macromolecular structure determination. Acta Crystallogr. D Biol. Crystallogr. *54*, 905–921.

Carman, C.V., Jun, C.D., Salas, A., and Springer, T.A. (2003). Endothelial cells proactively form microvilli-like membrane projections upon intercellular adhesion molecule 1 engagement of leukocyte LFA-1. J. Immunol. *171*, 6135–6144.

Carson, M. (1995). Ribbons. In Methods in Enzymology, C.W. Carter, Jr., and R.M. Sweet, eds. (San Diego: Academic Press), pp. 493–505.

Casasnovas, J.M., Stehle, T., Liu, J.-H., Wang, J.-H., and Springer, T.A. (1998). A dimeric crystal structure for the N-terminal two domains of intercellular adhesion molecule-1. Proc. Natl. Acad. Sci. USA *95*, 4134–4139.

de Fougerolles, A.R., and Springer, T.A. (1992). Intercellular adhesion molecule *3*, a third adhesion counter-receptor for lymphocyte function-associated molecule 1 on resting lymphocytes. J. Exp. Med. *175*, 185–190.

Diamond, M.S., Staunton, D.E., Marlin, S.D., and Springer, T.A. (1991). Binding of the integrin Mac-1 (CD11b/CD18) to the third immunoglobulin-like domain of ICAM-1 (CD54) and its regulation by glycosylation. Cell *65*, 961–971.

Fawcett, J., Holness, C.L., Needham, L.A., Turley, H., Gatter, K.C., Mason, D.Y., and Simmons, D.L. (1992). Molecular cloning of ICAM-3, a third ligand for LFA-1, constitutively expressed on resting leukocytes. Nature *360*, 481–484.

Gahmberg, C.G. (1997). Leukocyte adhesion: CD11/CD18 integrins and intercellular adhesion molecules. Curr. Opin. Cell Biol. *9*, 643–650.

Grakoui, A., Bromley, S.K., Sumen, C., Davis, M.M., Shaw, A.S., Allen, P.M., and Dustin, M.L. (1999). The immunological synapse: a molecular machine controlling T cell activation. Science *285*, 221–227.

Hamada, K., Shimizu, T., Yonemura, S., Tsukita, S., and Hakoshima, T. (2003). Structural basis of adhesion-molecule recognition by ERM proteins revealed by the crystal structure of the radixin-ICAM-2 complex. EMBO J. *22*, 502–514.

Huppa, J.B., and Davis, M.M. (2003). T-cell-antigen recognition and the immunological synapse. Nat. Rev. Immunol. *3*, 973–983.

Hynes, R.O. (2002). Integrins: bidirectional, allosteric signaling machines. Cell *110*, 673–687.

Jones, T.A., Zou, J.-Y., Cowan, S.W., and Kjeldgaard, M. (1991). Improved methods for building protein models in electron density maps and location of errors in these models. Acta Crystallogr. A *47*, 110–119.

Jun, C.D., Carman, C.V., Redick, S.D., Shimaoka, M., Erickson, H.P., and Springer, T.A. (2001a). Ultrastructure and function of dimeric, soluble intercellular adhesion molecule-1 (ICAM-1). J. Biol. Chem. *276*, 29019–29027.

Jun, C.D., Shimaoka, M., Carman, C.V., Takagi, J., and Springer, T.A. (2001b). Dimerization and the effectiveness of ICAM-1 in mediating LFA-1- dependent adhesion. Proc. Natl. Acad. Sci. USA *98*, 6830–6835.

Kirchhausen, T., Staunton, D.E., and Springer, T.A. (1993). Location of the domains of ICAM-1 by immunolabeling and single-molecule electron microscopy. J. Leukoc. Biol. *53*, 342–346.

Lee, K.H., Dinner, A.R., Tu, C., Campi, G., Raychaudhuri, S., Varma, R., Sims, T.N., Burack, W.R., Wu, H., Wang, J., et al. (2003). The immunological synapse balances T cell receptor signaling and degradation. Science *302*, 1218–1222.

Miller, J., Knorr, R., Ferrone, M., Houdei, R., Carron, C.P., and Dustin, M.L. (1995). Intercellular adhesion molecule-1 dimerization and its consequences for adhesion mediated by lymphocyte function associated-1. J. Exp. Med. *182*, 1231–1241.

Otwinowski, Z., and Minor, W. (1997). Processing of X-ray diffraction data collected in oscillation mode. In Macromolecular Crystallography, C.W. Carte, Jr., and R.M. Sweet, eds. (San Diego: Academic Press), pp. 307–326.

Reilly, P.L., Woska, J.R., Jr., Jeanfavre, D.D., McNally, E., Rothlein, R., and Bormann, B.J. (1995). The native structure of intercellular adhesion molecule-1 (ICAM-1) is a dimer. Correlation with binding to LFA-1. J. Immunol. *155*, 529–532.

Shimaoka, M., Xiao, T., Liu, J.H., Yang, Y., Dong, Y., Jun, C.D., McCormack, A., Zhang, R., Joachimiak, A., Takagi, J., et al. (2003). Structures of the αL I domain and its complex with ICAM-1 reveal a shape-shifting pathway for integrin regulation. Cell *112*, 99–111.

Springer, T.A. (1990). Adhesion receptors of the immune system. Nature *346*, 425–434.

Staunton, D.E., Dustin, M.L., Erickson, H.P., and Springer, T.A. (1990). The arrangement of the immunoglobulin-like domains of ICAM-1 and the binding sites for LFA-1 and rhinovirus. Cell *61*, 243–254.

Terwilliger, T.C., and Berendzen, J. (1999). Automated MAD and MIR structure solution. Acta Crystallogr. D Biol. Crystallogr. *55*, 849–861.

Vazeux, R., Hoffman, P.A., Tomita, J.K., Dickinson, E.S., Jasman, R.L., St. John, T., and Gallatin, W.M. (1992). Cloning and characterization of a new intercellular adhesion molecule ICAM-R. Nature *360*, 485–488.

Voraberger, G., Schafer, R., and Stratowa, C. (1991). Cloning of the human gene for intercellular adhesion molecule 1 and analysis of its 5′-regulatory region. Induction by cytokines and phorbol ester. J. Immunol. *147*, 2777–2786.

Wang, J.-H., and Springer, T.A. (1998). Structural specializations of immunoglobulin superfamily members for adhesion to integrins and viruses. Immunol. Rev. *163*, 197–215.

Accession Numbers

The coordinates of the ICAM-1 D3–D5 fragment have been deposited in Protein Data Bank with the code 1P53.